Independent isotopic fission yields of ^{252}Cf spontaneous fission via mass measurements at the FRS Ion Catcher

Y. Waschitz[1,], *D.* Amanbayev[2,], *A.* Spătaru[3,4,], *I.* Mardor[5,6,*], *T.* Dickel[7,2,], *E. O.* Cohen[8,], *O.* Aviv[6,], *S.* Ayet San Andrés[7,2,], *D. L.* Balabanski[3,], *S.* Beck[7,2,], *J.* Bergmann[2,], *Z.* Brencic[9,], *P.* Constantin[3,], *M.* Dehghan[7,], *H.* Geissel[7,2,], *L.* Gröf[2,], *C.* Hornung[7,], *N.* Kalantar-Nayestanaki[10,], *G.* Kripko-Koncz[2,], *I.* Miskun[2,], *A.* Mollaebrahimi[10,2,], *D.* Nichita[3,4,], *W. R.* Plaß[7,2,], *S.* Pomp[11,], *C.* Scheidenberger[7,2,12,], *A.* Solders[11,], *G.* Stanic[13,7,], *M.* Wasserheß[2,], *M.* Vencelj[9,], and *J.* Zhao[7,]

[1]Israel Atomic Energy Commission, P.O. Box 7061, Tel Aviv 61070, Israel
[2]II. Physikalisches Institut, Justus-Liebig-Universität Gießen, 35392 Gießen, Germany
[3]Extreme Light Infrastructure-Nuclear Physics (ELI-NP), Horia Hulubei National Institute for R&D in Physics and Nuclear Engineering, Str. Reactorului 30, 077125 Bucharest-Măgurele, Romania
[4]Doctoral School in Engineering and Applications of Lasers and Accelerators, University Polytechnica of Bucharest, 060811 Bucharest, Romania
[5]Soreq Nuclear Research Center, Yavne 81800, Israel
[6]School of Physics and Astronomy, Tel Aviv University, Tel Aviv 6997801, Israel
[7]GSI Helmholtzzentrum für Schwerionenforschung GmbH, 64291 Darmstadt, Germany
[8]Department of Physics, Nuclear Research Center Negev, P.O. Box 9001, Beer Sheva 84190, Israel
[9]Jozef Stefan Institute, SI-1000 Ljubljana, Slovenia
[10]Nuclear Energy Group, ESRIG, University of Groningen, 9747 AA Groningen, The Netherlands
[11]Department of Physics and Astronomy, Uppsala University, SE-75105 Uppsala, Sweden
[12]Helmholtz Forschungsakademie Hessen für FAIR (HFHF), GSI Helmholtzzentrum für Schwerionenforschung, Campus Gießen, 35392 Gießen, Germany
[13]Johannes Gutenberg-Universität Mainz, 55099 Mainz, Germany

Abstract. We present first preliminary results of a novel method for measuring independent isotopic fission yields (IIFYs) of spontaneous fission (SF) via direct mass measurements, at the FRS Ion Catcher (FRS-IC) at GSI. Fission products were generated from a ^{252}Cf source installed in a cryogenic stopping cell, and were identified and counted with the multiple-reflection time-of-flight mass spectrometer (MR-TOF-MS) of the FRS-IC, utilizing well-established measurement and data analysis methods. The MR-TOF-MS resolves isobars unambiguously, even with limited statistics, and its non-scanning nature ensures minimal relative systematic uncertainties amongst fission products. The analysis for extracting IIFYs includes isotope-dependent efficiency corrections for all components of the FRS-IC. In particular, we applied a self-consistent technique that takes into account the element-dependent survival efficiencies in the CSC, due to chemical reactions with the buffer gas. Our IIFY results, which cover several tens of fission products in the less-accessible high-mass peak (Z = 56 to 63) down to fission yields at the level of 10^{-5}, are generally similar to those of the nuclear database ENDF/B-VII.0. Nevertheless, they reveal some structures that are not observed in the database smooth trends. These are the first results of a planned campaign to investigate IIFY distributions of spontaneous fission at the FRS-IC. Upcoming experiments will extend our results to wider Z and N ranges, lower fission yields, and other spontaneously-fissioning actinides.

1 Introduction

The nuclear fission process has wide basic and applied science implications, including nuclear structure and reactions [1], the abundance of elements through nucleosynthesis [2], and nuclear waste management and safety [3]. Measurements of independent isotopic fission yields (IIFYs) provide access to the probability distribution of fission products, which contribute to understanding nuclear fission in more depth than mass yield distributions [1].

There exist two main experimental techniques to measure IIFYs in direct kinematics, but as described in the following, they are not universal and can be applied only to certain fission products.

Fission products can be identified by the characteristic γ-rays of their radioactive decay [4]. However, in most cases this method is useful mainly for cumulative fission yields, namely the yields following subsequent β-decay stages. In addition, this method is less effective for fission products whose gamma-line information is limited or

*e-mail: mardor@tauex.tau.ac.il

non-existent, have very short or very long half-lives, or are stable isotopes [1].

At the Lohengrin recoil separator [5] in the high-flux reactor of the ILL (Grenoble, France), products of thermal-neutron-induced fission are separated in-flight by an ion-optical system that determines their mass. The nuclear-charge is obtained by the ΔE-E method with a split-anode ionization chamber, but due to the fission products low kinetic energy, it can resolve isotopes only up to Z≈42, so it covers only the light-mass peak. In the heavy-mass peak, isotopic yields are determined by γ-ray spectrometry [6], with the inherent limitations described in the previous paragraph.

Therefore, a complementary method for measuring isotopic fission yields was called for, which should depend on unambiguous universal fission product identification. The International Atomic Energy Agency (IAEA) recommended in 2016 to pursue fission yield measurements via direct ion counting [3], which was introduced in 2010 by Pentillä and co-workers at JYFLTRAP for proton-induced fission of ^{nat}U [7, 8].

We recently demonstrated a method to measure isotopic yields of spontaneous fission (SF) [9] via direct ion counting at the FRS Ion Catcher (FRS-IC) at GSI [10], utilizing its high-resolving multiple-reflection time-of-flight mass-spectrometer (MR-TOF-MS) [11]. Measurements of SF properties are important for the basic understanding of fission, since the fission process takes place at a specific excitation energy, which enables to benchmark theories. This method can be applied also for neutron-induced fission at various incoming neutron energies, e.g., at the Soreq Applied Research Accelerator Facility (SARAF) [12], currently under construction in Yavne, Israel.

In this proceedings, we briefly recall the measurement technique, describe our analysis procedure to determine isotopic fission yields from our measurements with a ^{252}Cf source, present our first preliminary results, and give an outlook to our future plans.

2 The measurement technique

The measurement is performed at the FRS-IC [10] in GSI/FAIR (Darmstadt, Germany). A SF source is installed inside a cryogenic stopping cell (CSC) [13–15]. The fission products (FPs) are thermalized in the CSC buffer gas and are then extracted, diagnosed and transported by a versatile RFQ beam-line [16]. They are identified via accurate mass measurement by a MR-TOF-MS, which can separate isobars and thus provide unambiguous identification of the FPs [11]. The amount of each FP is extracted by a well-established fitting technique that takes into account also overlapping peaks [17]. For more details on the measurement technique, see [9].

3 First experimental campaign

The first experimental campaign for measuring SF yields at the FRS-IC was performed with the standard configuration of the CSC, which is optimized for thermalizing incoming relativistic ions. The SF source was placed 9 cm off-axis (see Fig. 1). The active dimensions of the CSC are a length of 98 cm and a radius of 12.5 cm.

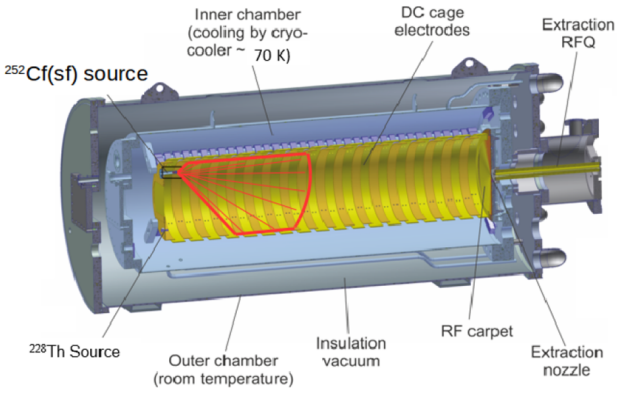

Figure 1. Cross section of the CSC with the internal long DC cage that is optimized for thermalizing relativistic ions. The ^{252}Cf SF source is installed at the upstream side of the CSC, 9 cm off-axis. The red lines mark the approximate range of the emitted FPs in the buffer gas.

In this experiment, the CSC was operated at a temperature of 90K and a pressure of 75 mbar. The extraction time from the CSC towards the MR-TOF-MS was less than 200 ms. The elements investigated were from the high-mass peak of the ^{252}Cf SF fission distribution, in the range Z=56 to 62, all of which are extracted as doubly-charged ions. The mass range of the extracted ions was from A=142 to 161. Recall that standard IIFY methods are usually limited to the low-mass peak, up to Z≈42 (Section 1, [1]). The activity of the ^{252}Cf SF source during the experiment was approximately 20 kBq.

The mass resolving power (MRP) of the MR-TOF-MS at the FRS-IC can reach up to 1,000,000 [18]. However, for measuring fission yields a broadband mode was preferred, covering approximately 10 amu/e with an MRP of 320,000, corresponding to a flight time of approximately 9 ms in the MR-TOF-MS. A typical time-of-flight spectrum from this experiment is given in Fig. 2. FPs are identified by converting the time-of-flight to mass-over-charge and comparing to literature masses in the measured range [17].

4 The analysis method

To extract IIFYs from the experimental data, global and FP-dependent efficiency factors need to be evaluated and applied to the raw number of counts in the mass peaks. In this section, we outline these factors and describe the calculation or estimation for each of them.

4.1 Stopping efficiency

The stopping efficiency depends on the FP ranges in the Ti foil that covers the ^{252}Cf SF source and the He buffer gas. These ranges are different for each FP, since they depend on its mass and kinetic energy. Typical kinetic energies are assigned to each pair of FPs via energy and momentum

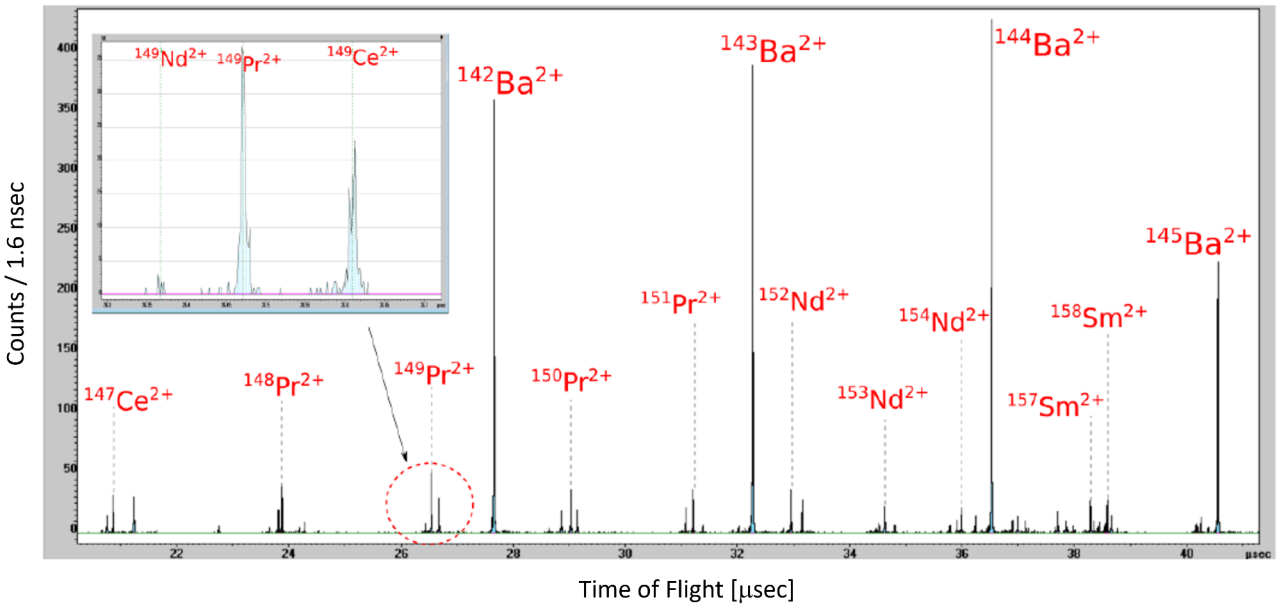

Figure 2. Typical time-of-flight spectrum during this experiment. All identified FPs are doubly charged and marked on the plot. The MRP is 320,000. The inset shows the clear separation between three A=149 isobars.

conservation, assuming binary fission from ^{252}Cf and no prompt neutrons and gammas. The range for all FPs in Ti and He gas was calculated via the code ATIMA [19]. The overall stopping efficiency of a FP in the CSC is a product of the emission efficiency from the Ti-covered source and geometrical efficiency due to the dimensions of the CSC.

Emission efficiency: The ^{252}Cf SF source was covered by a 4 μm thick Ti foil, to reduce the FPs kinetic energy, thus decreasing their range in the He buffer gas and increasing their stopping efficiency. Above a certain opening angle, an FP will be stopped in the foil. This opening angle defines the solid angle within which the FP propagates into the CSC He buffer gas. The emission efficiency is the ratio between this solid angle and 4π.

Geometrical efficiency: Given that the FP was emitted into the He buffer gas, it can either be stopped in the buffer gas and then extracted and measured, or be absorbed in the CSC walls and then be lost. The geometrical efficiency is the ratio between the three-dimensional surface composed of all points where a FP stops within the He buffer gas, and the three-dimensional surface defined by the FP range in He and the emission solid angle from the Ti-covered source. An illustration of the geometrical efficiency of a specific FP, ^{116}Pd, is given in Fig. 3.

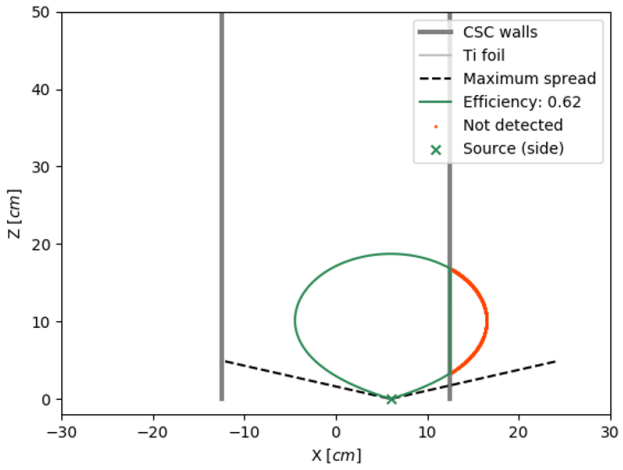

Figure 3. An illustration of the geometrical efficiency concept for the FP ^{116}Pd. The ^{252}Cf SF source is marked by ×. The dashed lines represent the opening angle in which ^{116}Pd is emitted to the He buffer gas, due to its range in Ti. The contour is a 2D cross section of the 3D surface defined by the range of ^{116}Pd in He. The green part is inside the He buffer gas, and the red part is beyond the CSC walls (vertical gray lines), marking the lost ^{116}Pd FPs. The geometrical efficiency is the ratio between the green and green+red **3D surfaces**, 62% in this case.

4.2 Global extraction, transport and detection efficiency

When a certain amount of FPs is stopped at the He buffer gas in the CSC, the amount that will eventually be counted in the MR-TOF-MS is lowered due to several efficiency parameters. In this Subsection, we describe the various global efficiencies at the FRS-IC.

Global efficiencies were evaluated by ^{224}Ra ions, which are α-recoil daughters of a ^{228}Th source with a known activity that is mounted on the upstream side of the CSC, 9 cm off-axis, just like the ^{252}Cf source (see Section 3 and Fig. 1). They were counted at various detection stations along the FRS-IC and compared to the known ^{228}Th source activity.

The efficiencies and transmissions that were taken into account are those of CSC extraction, RFQ beam line, MR-TOF-MS, MR-TOF-MS detector, and the Isolation-Dissociation-Isolation (IDI) process (breaking up of stable molecular ions that contaminate the signal [20]). ^{224}Ra

ions reach a doubly charged state in the CSC, so their results are representative of the measured FPs in this experiment, which are all doubly charged in the CSC as well.

4.3 Chemical efficiency

The FPs undergo chemical reactions with the He buffer gas and contaminants in the CSC and the residual gas in the rest of the FRS-IC, which lead to element-dependent (chemical) efficiencies. Unlike the efficiencies described in the previous Subsections, there is no model or independent measurement that we can perform to extract these efficiencies for all FPs. We present here a self-consistent method to extract the chemical parameters of the FRS-IC, which is inspired by a similar approach that was applied for proton-induced fission [8].

The chemical efficiencies can be obtained by the obvious assumption that they are the same for all FPs that are isotopes of the same element, and by constraining the sum of IIFYs of mass chains to the well-known mass yields of ^{252}Cf SF [21].

Since we did not measure the entire mass chain in any case, we constrain the sum of the IIFYs along a mass chain by a fraction of the mass-yield, where the fraction value is given by the ratio between the sum of the literature IIFY values of the measured FPs and the mass yield. These assumption and constraint lead to the following set of equations:

$$\sum_{Z} \mathrm{IIFY(N,Z)}_{\mathrm{exp}}^{\mathrm{N+Z=A}} \cdot \mathrm{C(Z)} = \mathrm{frac(A)} \cdot \mathrm{Y(A)}_{\mathrm{lit}}, \qquad (1)$$

where $\mathrm{IIFY(N,Z)}_{\mathrm{exp}}^{\mathrm{N+Z=A}}$ are the measured yields after taking into account the efficiency factors described in the previous Subsections, C(Z) are the inverses of the element dependent chemical efficiencies, $\mathrm{Y(A)}_{\mathrm{lit}}$ is the literature mass-yield of the mass chain A, and frac(A) is defined as:

$$\mathrm{frac(A)} \equiv \frac{\sum_{meas} \mathrm{IIFY(N,Z)}_{\mathrm{lit}}^{\mathrm{N+Z=A}}}{\mathrm{Y(A)}_{\mathrm{lit}}}. \qquad (2)$$

Mathematically, $\mathrm{Y(A)}_{\mathrm{lit}}$ cancels out in Eq. 1. Nevertheless, we keep this representation to emphasize the equation's context. Along each mass chain, the IIFYs are reduced by about an order of magnitude for each increasing and decreasing Z value away from the fission yield peak. Therefore, the value of frac(A) is usually quite high even if only the few nuclei with the highest yield are measured in a mass chain. This means that the specific values of $\mathrm{IIFY(N,Z)}_{\mathrm{lit}}^{\mathrm{N+Z=A}}$ have hardly any bias on the determination of C(Z) values, since only their sums are used, and they are very close to the $\mathrm{Y(A)}_{\mathrm{lit}}$ values that are well-known experimentally.

The nuclei for which we measured IIFY values are marked on the nuclear chart in Fig. 4. As can be seen, from these measurements we can construct a set of 17 equations like Eq. 1, which are enough for the extraction of 8 chemical efficiencies (Z= 56 to 63). The amounts of mass-chain members in the 17 equations vary between two and five. As expected, the frac(A) values are very high: above 99% for the 5- and 4-nuclei equations, above 91% for all 3-nuclei equations, between 68% and 90% for 2-nuclei equations. This emphasizes the minimal bias of $\mathrm{IIFY(N,Z)}_{\mathrm{lit}}^{\mathrm{N+Z=A}}$ values on our extraction of C(Z).

The set of equations in Eq. 1 is solved by searching for the C(Z) values that minimize χ^2 of the set, which is defined by:

$$\chi^2 = \sum_{A} \frac{(LHS(A) - RHS(A))^2}{\Delta LHS(A)^2 + \Delta RHS(A)^2}, \qquad (3)$$

where (LHS(A)) and (RHS(A)) are the left-hand and right-hand sides of each equation in set 1, respectively, and $\Delta LHS(A)$ and $\Delta RHS(A)$ are evaluated by propagating the uncertainties of their respective components.

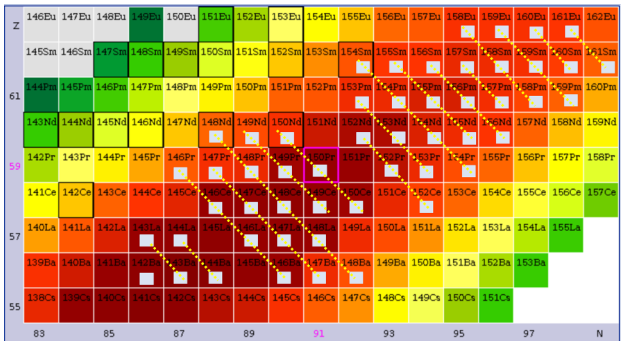

Figure 4. The nuclei for which IIFY values were determined in this experiment, depicted on the nuclear chart with a color code based on evaluated IIFYs for ^{252}Cf SF from ENDF/B-VII.0 [21]. The light gray squares mark the measured nuclei, and the yellow dashed lines mark the 17 equations from which we extract the inverse chemical efficiencies C(Z). The missing mass chains (A=145, 151) are due to the specific MR-TOF-MS settings when this data set was measured.

4.4 Nuclear decay corrections

Some of the FPs undergo nuclear decays to other FPs during the measurement process. This effect, which increases the amount of resultant FPs at the expense of decaying FPs, can be accounted for by applying the Bateman equations for decay chains. The most relevant decay mode is β decay, but for very neutron-rich FPs there is also β-delayed single- and multi-neutron emission. Furthermore, the FPs that are created in isomeric states can either undergo β decay or de-excite to the ground state via internal transition.

For almost all measured nuclei in this experiment (see Fig. 4), the nuclear decay half-lives are much longer than the ion extraction and measurement time, less than 200 ms. We therefore did not apply decay corrections within the analysis reported here.

There are also several known isomers within the measured nuclei, but either their excitation energy is below the MR-TOF-MS resolving limit in this experiment (approximately 300 keV), or their half-lives are in the μs and ns ranges, way below the extraction and measurement time. Therefore, in this experiment, for all isomers, the IIFY value is a sum of the ground and isomeric state values, and no isomer yield ratio is determined.

5 Preliminary results

The data analysis of the experiment is still ongoing. Here we present preliminary results for the isotopes of two elements, Ce (Z=58) and Nd (Z=60).

We present our results in Fig. 5. The open black circles are our results after applying only the global and FP-dependent efficiency and transmission corrections that were described in Subsections 4.1 and 4.2, i.e., before chemical corrections. Note that in this experiment the chemical corrections are especially large due to a cleanliness problem in the trap system of the MR-TOF-MS. Therefore, the chemical corrections are expected to be much smaller in future campaigns.

The reported uncertainties in the experimental values are only statistical ones, and depend directly on the number of events in the mass peaks. One can see that the neutron-number dependencies of these results are similar to those of ENDF/B-VII.0 [21] and JENDL-5 [22] evaluations and previous experimental data [23–26]. This implies that following our application of FP-dependent corrections, we get IIFY values that are correct up to a factor that is only element-dependent, with no additional neutron-number dependence.

When applying the self-consistent procedure described in Subsection 4.3, we obtain preliminary absolute IIFY values, marked by full black circles in Fig. 5.

The statistical uncertainties in these results (black markings) are due to the number of events in the mass peaks. The systematic uncertainties (magenta markings), which are in most cases larger than the statistical ones, are those of the fitting procedure for extracting the chemical efficiencies.

All the experiments reported in [23–26] identified FP pairs via detection of coincident triple- or quadruple-gamma rays using high-resolution spectroscopic detectors. The aim was to identify complementary FPs by their unique cascades (quadruple coincidence), or at least one by its cascade and the other by a single gamma line (triple coincidence).

There is consistency with most experimental results, except for several discrepancies with the results of [26]. Furthermore, almost all our results are consistent with the database evaluations, and most are measured with lower uncertainties. Since our results are still preliminary, we defer further investigation into the sources of the existing discrepancies until the completion of our data analysis.

6 Summary and outlook

In this paper, we present first preliminary IIFY results for SF of ^{252}Cf, measured by direct mass identification of the FPs at the FRS-IC. We outlined the data analysis method, describing how we take into account the various efficiencies and transmissions that are required for converting mass-peak amounts to IIFYs. Most measured IIFYs are consistent with database evaluations and previous experimental results (Fig. 5), thereby corroborating our analysis method, including the treatment of element-dependent chemical efficiencies.

We continue to analyze all the data that was acquired in the first experiment (Fig. 4). By comparing to additional data sets that were measured and synthetic data that we will generate by simulation, we plan to evaluate the limits of our method, e.g., what are the minimal amount of FPs in a mass-chain equation that we should use, the minimal value of the parameter frac(A) (Eq. 2), the effect of nuclei missing from the measurement, the reliability of chemical efficiencies at the proton-number edges of our sample, and more.

In parallel to the analysis effort, we plan to conduct more measurements, to cover more parts of the FP distribution. In the reported experiment, we reached IIFYs values down to the 10^{-5} range, with a 20kBq ^{252}Cf source. In future runs, we will be able to extend our reach to far lower fission yields, due to the improvements described below.

A short DC cage will be installed in the CSC, with a higher electric field and special instrumentation to install SF sources on-axis [27], which would increase the stopping and extraction efficiency by at least an order of magnitude. In addition, we plan to install a ^{252}Cf source with higher activity that will enable reaching lower fission yields, and possibly other SF sources that will enable systematic comparisons of different fissioning systems.

Acknowledgements

This work was supported by the German Research Foundation (DFG) Grant No. 57564554, by Justus-Liebig-Universität Gießen and GSI under the JLU-GSI strategic Helmholtz partnership agreement, by the Israel Ministry of Energy, Research Grant No. 220-11-052 and by the International Atomic Energy Agency, IAEA Research Contract No: 24000.

References

[1] A.N. Andreyev, K. Nishio, K.H. Schmidt, Reports on Progress in Physics **81**, 016301 (2017)

[2] G. Martínez-Pinedo, D. Mocelj, N. Zinner, A. Kelić, K. Langanke, I. Panov, B. Pfeiffer, T. Rauscher, K.H. Schmidt, F.K. Thielemann, Progress in Particle and Nuclear Physics **59**, 199 (2007), international Workshop on Nuclear Physics 28th Course

[3] P. Dimitriou, F.J. Hambsch, S. Pomp, IAEA INDC (NDS) **0713** (2016)

[4] H. Naik, S. Mukerji, R. Crasta, S. Suryanarayana, S. Sharma, A. Goswami, Nuclear Physics A **941**, 16 (2015)

[5] P. Armbruster, M. Asghar, J. Bocquet, R. Decker, H. Ewald, J. Greif, E. Moll, B. Pfeiffer, H. Schrader, F. Schussler et al., Nuclear Instruments and Methods **139**, 213 (1976)

[6] F. Martin, C. Sage, G. Kessedjian, O. Sérot, C. Amouroux, C. Bacri, A. Bidaud, A. Billebaud, N. Capellan, S. Chabod et al., Nuclear Data Sheets **119**, 328 (2014)

[7] H. Penttilä, P. Karvonen, T. Eronen, V.V. Elomaa, U. Hager, J. Hakala, A. Jokinen, A. Kankainen, I.D.

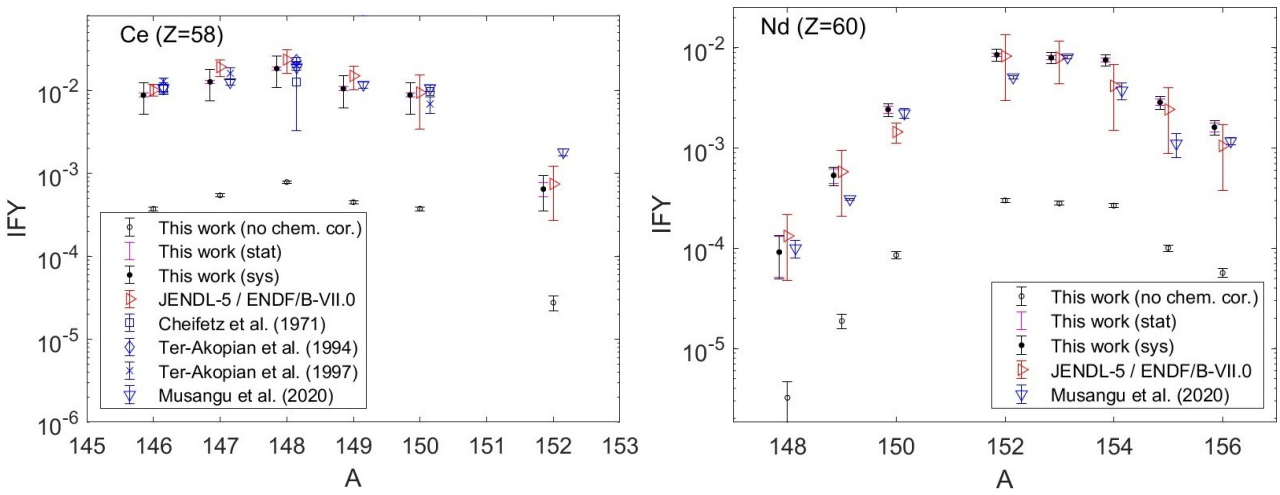

Figure 5. IIFY preliminary results for the measured isotopes of Ce (left) and Nd (right). Open black circles mark our results without chemical corrections), with uncertainties that are only statistical. Full black circles mark our results with all corrections applied, including the chemical efficiencies. Both statistical (black) and systematic (magenta) uncertainties are marked. The evaluations for these isotopes (red symbols) are identical in the ENDF/B-VII.0 [21] and JENDL-5 [22] databases. Previous experimental results are taken from [23–26].

Moore, K. Peräjärvi et al., The European Physical Journal A **44**, 147 (2010)

[8] H. Penttilä, D. Gorelov, V.V. Elomaa, T. Eronen, U. Hager, J. Hakala, A. Jokinen, A. Kankainen, P. Karvonen, I.D. Moore et al., The European Physical Journal A **52**, 104 (2016)

[9] Mardor, Israel, Dickel, Timo, Amanbayev, Daler, Ayet San Andrés, Samuel, Beck, Sönke, Benyamin, David, Bergmann, Julian, Constantin, Paul, Cléroux Cuillerier, Alexandre, Geissel, Hans et al., EPJ Web Conf. **239**, 02004 (2020)

[10] W.R. Plaß, T. Dickel, S. Purushothaman, P. Dendooven, H. Geissel, J. Ebert, E. Haettner, C. Jesch, M. Ranjan, M.P. Reiter et al., NIM B **317**, 457 (2013)

[11] T. Dickel, W.R. Plaß, A. Becker, U. Czok, H. Geissel, E. Haettner, C. Jesch, W. Kinsel, M. Petrick, C. Scheidenberger et al., NIM A **777**, 172 (2015)

[12] I. Mardor, O. Aviv, M. Avrigeanu, D. Berkovits, A. Dahan, T. Dickel, I. Eliyahu, M. Gai, I. Gavish-Segev, S. Halfon et al., The European Physical Journal A **54**, 91 (2018)

[13] M. Ranjan, S. Purushothaman, T. Dickel, H. Geissel, W.R. Plaß, D. Schäfer, C. Scheidenberger, J.V. de Walle, H. Weick, P. Dendooven, Europhys. Lett. **96**, 52001 (2011)

[14] S. Purushothaman, M.P. Reiter, E. Haettner, P. Dendooven, T. Dickel, H. Geissel, J. Ebert, C. Jesch, W.R. Plaß, M. Ranjan et al., Europhys. Lett. **104**, 42001 (2013)

[15] M. Ranjan, P. Dendooven, S. Purushothaman, T. Dickel, M. Reiter, S. Ayet San Andrés, E. Haettner, I. Moore, N. Kalantar-Nayestanaki, H. Geissel et al., NIM A **770**, 87 (2015)

[16] E. Haettner, W. R. Plaß, U. Czok, T. Dickel, H. Geissel, W. Kinsel, M. Petrick, T. Schäfer, C. Scheidenberger, Nuclear Instruments and Methods in Physics Research Section A: Accelerators, Spectrometers, Detectors and Associated Equipment **880**, 138 (2018)

[17] S. Ayet San Andrés, C. Hornung, J. Ebert, W.R. Plaß, T. Dickel, H. Geissel, C. Scheidenberger, J. Bergmann, F. Greiner, E. Haettner et al., Phys. Rev. C **99**, 064313 (2019)

[18] I. Mardor, S. Ayet San Andrés, T. Dickel, D. Amanbayev, S. Beck, J. Bergmann, H. Geissel, L. Gröf, E. Haettner, C. Hornung et al., Phys. Rev. C **103**, 034319 (2021)

[19] H. Weick, H. Geissel, N. Iwasa, C. Scheidenberger, J.L.R. Sanchez, A. Prochazka, S. Purushothaman, the Super-FRS experiment collaboration, GSI Sci. Rep. 2017 (2018)

[20] F. Greiner, T. Dickel, S. Ayet San Andrés, J. Bergmann, P. Constantin, J. Ebert, H. Geissel, E. Haettner, C. Hornung, I. Miskun et al., Nuclear Instruments and Methods in Physics Research Section B: Beam Interactions with Materials and Atoms **463**, 324 (2020)

[21] *ENDF/B-VII.0 data extracted from: National Nuclear Data Center, NuDat 3 database*, https://www.nndc.bnl.gov/nudat3/

[22] Iwamoto, Osamu, Iwamoto, Nobuyuki, Shibata, Keiichi, Ichihara, Akira, Kunieda, Satoshi, Minato, Futoshi, Nakayama, Shinsuke, EPJ Web Conf. **239**, 09002 (2020)

[23] E. Cheifetz, J.B. Wilhelmy, R.C. Jared, S.G. Thompson, Phys. Rev. C **4**, 1913 (1971)

[24] G.M. Ter-Akopian, J.H. Hamilton, Y.T. Oganessian, J. Kormicki, G.S. Popeko, A.V. Daniel, A.V. Ramayya, Q. Lu, K. Butler-Moore, W.C. Ma et al., Phys. Rev. Lett. **73**, 1477 (1994)

[25] G.M. Ter-Akopian, J.H. Hamilton, Y.T. Oganessian, A.V. Daniel, J. Kormicki, A.V. Ramayya, G.S. Popeko, B.R.S. Babu, Q.H. Lu, K. Butler-Moore et al., Phys. Rev. C **55**, 1146 (1997)

[26] B.M. Musangu, A.H. Thibeault, T.H. Richards, E.H. Wang, J.H. Hamilton, C.J. Zachary, J.M. Eldridge, A.V. Ramayya, Y.X. Luo, J.O. Rasmussen et al., Phys. Rev. C **101**, 034610 (2020)

[27] A. Rotaru, D. Amanbayev, D.L. Balabanski, D. Benyamin, P. Constantin, T. Dickel, L. Gröf, I. Mardor, I. Miskun, D. Nichita et al., Nuclear Instruments and Methods in Physics Research Section B: Beam Interactions with Materials and Atoms **512**, 83 (2022)